

Air–sea interaction under low and moderate winds in the Black Sea coastal zone

Irina Repina^{a,b,c}, Arseny Artamonov^a, Alexander Chukharev^d, Igor Esau^{e,f},
Yury Goryachkin^d, Alexey Kuzmin^b, Michael Pospelov^b, Ilya Sadovsky^{b,g}
and Mikhail Smirnov^h

^a A. M. Obukhov Institute of Atmospheric Physics RAS, Pyzhevski per. 3, 119017 Moscow, Russia; repina@ifaran.ru

^b Space Research Institute, Profsoyuznaya Str. 84/32, 117997 Moscow, Russia

^c Russian State Hydrometeorological University, Malookhtinsky prospect 98, 195196 Saint-Petersburg, Russia

^d Marine Hydrophysical Institute NASU, Kapitanskaya St. 2, 99011 Sevastopol, Ukraine

^e Nansen Environmental and Remote Sensing Centre, G. C. Rieber Climate Institute, Thormøhlens gate 47, N-5006 Bergen, Norway

^f Centre for Climate Dynamics (SKD), Allegaten 70, N-5007 Bergen, Norway

^g Vladimir State University, Gorkogo 87, 600000 Vladimir, Russia

^h A. V. Kotelnikov Institute of Radioengineering and Electronics RAS, Vvedensky Sq. 1, 141120 Fryazino, Moscow region, Russia

Received 23 March 2012, in revised form 16 May 2012

Abstract. This paper reports the results of field experiments performed at an offshore oceanographic platform in the Black Sea during spring and fall seasons 2005–2011. Observations of the air–sea interaction were made using direct and remote sensing methods in the coastal zone where the interaction is complex and still poorly understood. A specialized research platform, managed by the Marine Hydrophysical Institute (MHI), is placed on the shelf slope approximately 600 m offshore the Crimea coast, Ukraine. The water depth at the site is about 30 m. The experiment program included conventional turbulence measurements with the eddy-covariance method as well as remote radio-polarimetric measurements with a newly developed instrument. The study was concentrated on the air–sea interaction during episodes of weak wind in the atmosphere and upwelling events in the ocean. Analysis of the collected data confirmed significant dependence of the surface drag coefficient on the air–sea temperature difference under weak wind conditions. However, this analysis also demonstrated a new air–sea interaction regime, which is characterized by large quasi-periodic (periods about 3.5 h) turbulence oscillations developing initially in the atmosphere and later (after about 10–12 h) in the sub-surface water layer. The analysis of radio-polarimetric measurements provided the characteristics of the gravity-capillary wave field during these events.

Key words: coastal zone, atmospheric boundary layer, sea drag coefficient, gravity-capillary wave, radio-polarimetric measurements.

1. INTRODUCTION

Air–sea interaction in the ocean coastal zone is driven by complex processes and usually enhanced due to additional energy input from the horizontal heterogeneity of the surface, upwelling and wave breaking. Despite a long tradition and numerous field experiments in the coastal zone ([^{1–3}]), details of these processes are still poorly understood. The relevant gaps result in systematic large uncertainties and biases in the coastal zone surface fluxes as revealed by the analysis of the compiled data sets ([^{4,5}]). Biases in the surface exchange coefficients have a considerable impact on the ability of models to reproduce the present-day climate and its decadal variability ([⁶]). Particularly significant difficulties arise under weak wind and stable-stratification conditions, which are rarely observed over the open ocean but rather common in the coastal zones on inland seas ([⁷]).

To narrow the gaps in the knowledge of air–sea interactions in the coastal zone, a series of field experiments was run from a sea-mounted platform in the coastal area of the Black Sea. The experiments were organized by the Experimental Department of the Marine Hydrophysical Institute of the Ukrainian National Academy of Science in 2005–2011. The platform (Fig. 1) is located offshore in Crimea (near town Katsiveli, 44°23′38″ N, 33°59′15″ E). It was built in 1980 and since then remains a unique research infrastructure to run a variety of



Fig. 1. Offshore oceanographic platform in the Black Sea, Katsiveli, Crimea coast, Ukraine.

meteorological and oceanographic studies in the Black Sea [8–11]. The platform's location at a distance of approximately 450–600 m from the coast and the water depth at this location (about 30 m) make it a unique observational point to collect the data in the coastal zone in an area that is usually unresolved in remote sensing data sets. Predominant winds at this site are from open sea sector of the bay (from eastern, western and southern directions). The predominant winds excite waves, which characteristics are similar to those of the well-developed waves in the open deep sea. Moreover, this part of the Black Sea is known for frequent coastal upwellings (caused by the forcing by persistent winds) and other non-stationary processes in autumn and spring seasons. It leads to diversity of the air–sea interaction regimes, which vary from strongly stratified conditions in the coupled boundary layers under upwelling events to strongly convective conditions during cold season [12,13].

2. INSTRUMENTATION AND METHODS

The field experiments were conducted by several groups from MHI (Ukraine), Space Research Institute (Russia), Vladimir State University (Russia), A. V. Kotelnikov Institute of Radioengineering and Electronics (Russia), and A. M. Obukhov Institute for Atmospheric Physics (Russia). The data collection was completed mostly during hydrological spring season (May through June). This season is characterized by intensive warming of the ocean mixed layer and the formation of a seasonal thermocline [14]. These processes have larger pace in the coastal zone due to more intensive vertical mixing, caused by wave breaking. A significant impact of the coastal upwelling, forced by persistent wind, was also recognized [15].

The largest part of data was collected during upwelling events in 2005 [9], while in 2009 and 2011, the data were collected in October during strong storms and vertical convection. The data were collected with instruments presented in Table 1. In order to minimize the effect of the platform constructions on measurements, the equipment was placed on 4–6 m long beams, which extend out of the sea-looking side of the platform. In addition, characteristics of the ocean mixed layer turbulence were measured with the “Sigma-1” instrument, developed by MHI [16]. This instrument collects data with a high frequency. It gives the possibility to retrieve patterns of spatio-temporal variability of the turbulence field under non-stationary meteorological conditions and for the changing wave field [17].

The turbulent fluxes of momentum, heat, humidity and CO₂ were obtained using the eddy-correlation method, which calculates the fluxes using co-variations between pulsations of measured parameters (see [18,19]). The flux is positive when it is directed upwards. This method involves certain assumptions about the statistical structure of the turbulence field but, in reward, it is applicable to observations over diverse surfaces. Additional spectral analysis was used to control the quality of pulsation measurements.

Table 1. Instruments and data set

Instrument	Measured parameters	Time interval	Location of measurements
Flow velocimeter “Vostok-M” (MHI-1306)	Module of current velocity V_R Azimuth of the device Temperature Relative conductivity Pressure	Sampling interval for all the channels is 15, 30 or 60 s	Depth 3, 5, 10, 15 and 20 m
MHI-4102 CTD probe (ISTOK)	Conductivity (salinity), temperature, pressure of sea water	1 h	Profile from surface to bottom
CTD probe FSI	Conductivity (salinity), temperature, pressure of sea water, current velocity	60 s	Depth 0.5 m
Water temperature sensor	Temperature of sea water	1 s	Depth 1 m
Position sea turbulence measuring complex “Sigma-1”	3-D velocity fluctuations Temperature Temperature fluctuations Relative conductivity Conductivity fluctuations Inclinations of the device Azimuth of the device Pressure	Sampling frequency of mean values is 20 Hz, fluctuations – 100 Hz	Depth 1–0.3 m
CTD probe YSI 30	Conductivity (salinity) and temperature of upper layer sea water	0.5 h	Depth 0.1 m
Gill WindSonic™ 2-axis ultrasonic anemometer	Horizontal components of the wind speed (u, v)	4 Hz	0.5 m
6- and 5-string wave gauges	Sea surface elevation	10 Hz	4 m
METEK ultrasonic anemometer USA-1	Wind vector and air temperature fluctuations	10 Hz	4 m
LI-COR 7500 gas analyser	Fluctuations of CO ₂ and H ₂ O concentrations, air pressure	10 Hz	4 m
A set of microwave and IR radiometers mounted on an automatic rotator “Travers”	Microwave (8, 1.5, 0.8 and 0.3 cm) and infrared radiation of sea surface	3 Hz	4 m
Meteorological station MK-15	Air temperature, wind direction and velocity	3 Hz	1.5 m, 21 m
Two-level automatic weather station AWS 2700 AANDERAA	Air temperature and humidity, wind direction and velocity, air pressure	60 s	5 m, 10 m
Video camera	Sea surface state	25 Hz	10 m
L-band radiometer	Microwave radiation (21 cm)		12 m
Digital photo camera Olympus 8080 WZ	Picture of the sea surface	15 min	12 m

In addition to traditional turbulence measurements (both in the atmosphere and under the sea surface), the experiments gathered data to study the evolution of gravity-capillary waves (GCW). This is the least studied part of the sea wave fields. In order to contribute to the understanding of the GCW, a new remote radio-polarimetric measurement method has been implemented. This method, the so-called Non-linear Radio-thermal Resonant Spectroscopy (NRRS), has been proposed in [20]. The physical principle of this method relates the microwave brightness temperature of the sea surface with the water temperature and emissivity. The latter depends on sea water permittivity and the geometry of the wavy surface. It has been shown [21–23] that microwave measurements using wavelengths of 0.3–1.5 cm are able to recover the surface wave spectrum in the range of wavelengths between 0.15 and 30 cm (wave numbers 0.2–42 rad/cm).

3. RESULTS

3.1. Surface drag coefficients

The surface drag coefficient, C_D , is one of the primary parameters required by the models of the air–sea interaction. This parameter determines turbulent stress (friction) over flat homogeneous but aerodynamically rough surface. It was studied in numerous works ([5,24–26], which cover the range of moderate and strong wind speeds ($5 < U_{10} < 25$ m/s, where U_{10} is the wind speed measured at the standard height of 10 m above the mean sea surface). The behaviour of these parameters outside this interval is known much less and a great deal of controversy and confusion does exist ([27,28]).

Analysis in this study was performed on a subset of data, limited to the interval of the air–sea temperature differences, ΔT , from -7 to $+12$ K and to the wind speed less than 15 m/s. The surface drag coefficient, C_D , was calculated using the observations of the wind speed, U_{10} , at 10 m height above the mean sea level, and the measured surface turbulent momentum flux (friction velocity) $\tau_{\text{turb}} = \rho_a u_*^2$. The dependence reads

$$C_D = \frac{\tau_{\text{turb}}}{\rho_a U_{10}^2} = \frac{u_*^2}{U_{10}^2}, \quad (1)$$

where ρ_a is the air density and u_* is the shear velocity.

Firstly, it is worth noting that the measured dependences of C_D on $(\Delta T, U_{10})$, which characterize the sensitivity of the air–sea interaction with respect to the stability of the surface atmospheric layer, are similar to those observed from different sea-mounted observational platforms around the world (e.g., [19,24,27]). Figure 2 shows $C_D(\Delta T)$ for weak, moderate and strong wind conditions. Figure 3 shows $C_D(U_{10})$ for three stability classes: $z/L < -0.05$ (unstable or convective conditions); $-0.05 < z/L < 0.05$ (near-neutrally stratified conditions); and $z/L > 0.05$ (stably-stratified conditions). The transition between convective

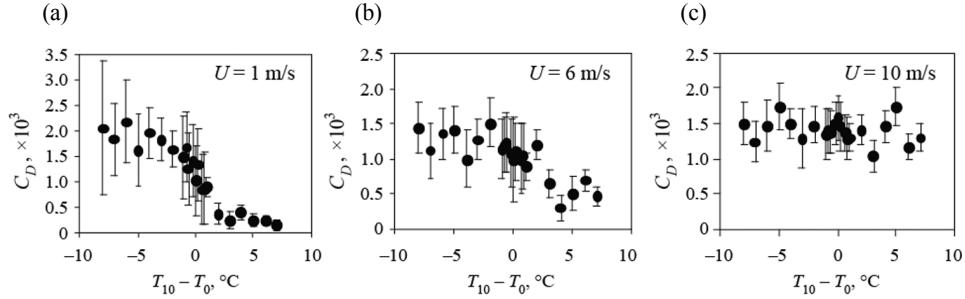


Fig. 2. Dependence between the surface temperature difference and the surface drag coefficient obtained using Eq. (1) for selected wind speed.

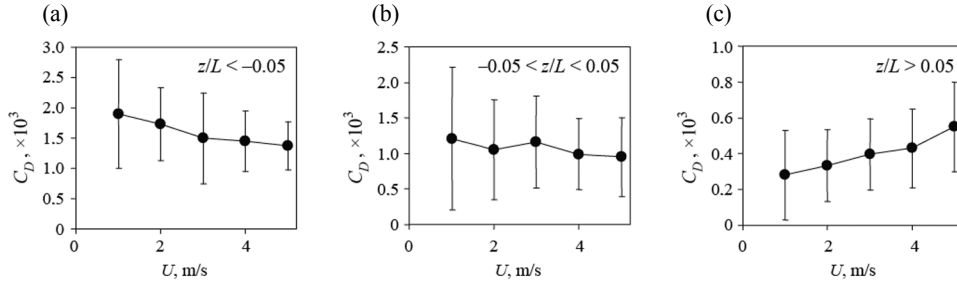


Fig. 3. Dependence between the wind speed and the surface drag coefficient obtained using Eq. (1) for three stability classes: unstable (a), neutral (b) and stable (c) conditions.

and stably stratified regimes of the vertical turbulent exchange is clearly seen for the weakest winds. This behaviour reminds the decoupling regime, described over the Baltic Sea in [7]. As it has been found before (e.g. [19]), the surface drag increases when the wind speed decreases under convective conditions. This behaviour was explained in [29] using the idea that convective winds, created by the self-organized turbulent motions, could be stronger than the observed mean wind. The contribution of the mean wind shear to the generation of near-surface turbulence, and therefore the surface drag, becomes relatively small. It makes the mean wind non-representative for the parameterization of the air-sea interaction under convective conditions.

The turbulence self-organization produces some contribution to the surface turbulent stress also in near-neutral conditions [30], but this contribution is significant only for weakly stratified atmosphere. There is no clear dependence of C_D on the wind speed in the near-neutral stability class. The value $C_D = 0.001$ is a commonly accepted value of the surface drag coefficient of the sea [24]. As the stably-stratified boundary layers are mixed by the mechanically generated turbulence, it is natural to expect that the surface turbulent stress will increase proportionally to U_{10} . Hence, one can expect that C_D will remain nearly constant for all wind speeds. Figure 3c shows that this is not the case. Under

stably-stratified conditions, $C_D(U_{10})$ is significantly reduced for the weakest winds. This fact could be explained by additional turbulence damping by the stable stratification [31]. In the stability class $0.05 < z/L$, the less stable cases are more frequent for larger U_{10} and the more stable cases – for smaller U_{10} . As C_D is the function of stability, given by z/L , this coarse classification may suggest a dependence on the wind speed, which could be a statistical artefact of the classification. In spite of this danger of misconception, the stability classes are still widely used in research and engineering literature ([32]).

3.2. Sea surface properties

The surface drag coefficient implicitly depends on the sea surface properties. In this experiment, the surface turbulent stress was measured. However, the turbulent stress is typically unknown in meteorological problems. It needs to be parameterized on the basis of a descriptive representation of the sea surface state. The convenient parameter is the surface roughness length, z_0 . In fact, it is a fitting parameter to minimize the difference between the observed and theoretical logarithmic velocity profiles [33]. Hence, it is mainly a property of the turbulent flow and not of the surface morphology: the same surface may have different values of z_0 for different flows. Nevertheless, it is convenient to use z_0 as a parameter describing the surface properties as well. In this experiment, the primary target to be studied is the spectra of surface gravity-capillary waves generated by the turbulent eddies imprinting on the surface. The field of GCW is a rather complex dynamical phenomenon, which evolution is sensitive to the wind speed, surface currents, internal waves in the upper sea layer, water depth, bathymetry, surface pollution, etc. [34,35]. Figure 4 shows how the stability of the flow depends on the surface drag coefficient and the surface roughness length scale, calculated using the experimental data set. The visually observed smoothing of the sea surface under stronger stratification is confirmed statistically by the associated decrease in z_0 .

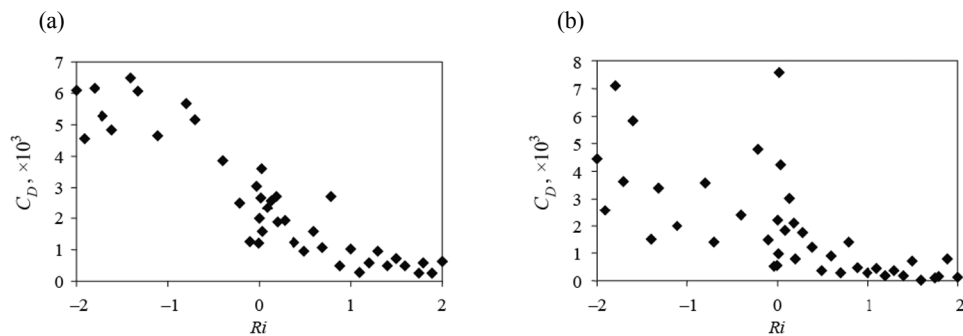


Fig. 4. Dependence of stability (expressed through surface bulk Richardson number) on the surface drag coefficient (a) and the surface roughness length scale (b).

The variations of the GCW spectra (Figs 5, 6) were obtained with a new NRRS (Non-linear Radio thermal Resonant Spectroscopy) method using a set of microwave radiometers (94.0, 37.5 and 20.0 GHz), mounted on an automatic rotator. Figure 5 shows an example of the parameters of a retrieved GCW spectrum under wind speed about 4 m/s. The experimental data are compared with several models of the ocean wave spectrum. The retrieval algorithm recovers the curvature spectrum (averaged on azimuth angle) and the long-wave's slope variance in the range of wave numbers of 0.389–15 rad/cm from angular radiometric measurements at a wavelength of 0.8 cm [20]. As the spectral plots are not convenient to study the temporal evolution of the GCW field, Fig. 6 shows this evolution for a few first wave numbers. When compared with the wind speed, the close correspondence between the GCW characteristics and the wind becomes obvious.

3.3. Oscillations in the air–sea turbulent exchange

Synchronous measurements of turbulent fluxes in the atmosphere and the upper ocean suggest that there exists some degree of coupling between the sub-sea turbulence and the atmospheric heat flux [36,37]. Here, we applied wavelet analysis to the data, collected during the experiment. Figure 7 reveals a new type of sub-mesoscale co-variability in the air–sea interactions. This co-variability is characterized by substantial variations in the turbulent kinetic energy on hourly time scales during the upwelling event. Their typical time scale is about 3.5 h.

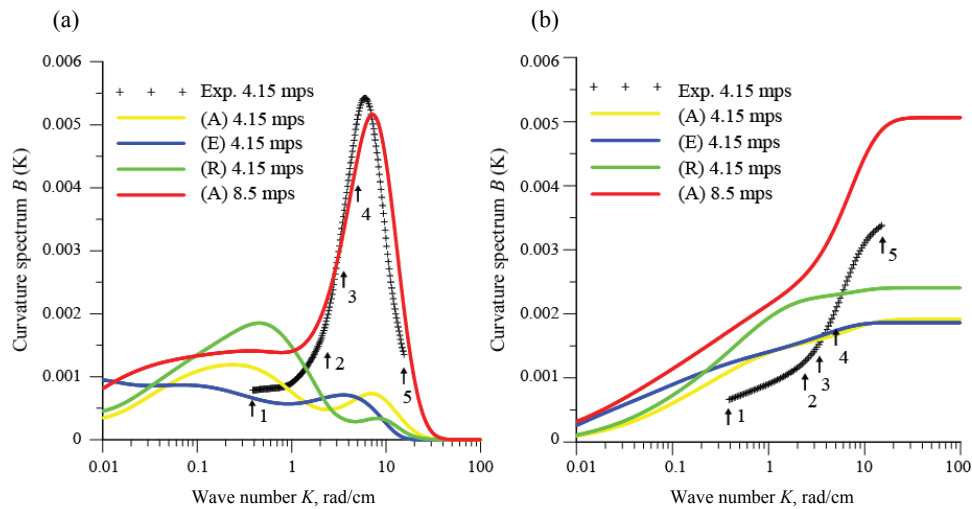


Fig. 5. An example of retrieved curvature function spectrum, averaged over azimuthal angle (a) and slope variance function (b) at wind velocity of 4 m/s, in comparison with some models of ocean wave spectrum. Exp – experimental data; A – model from [38]; E – model from [39]; R – model from [40].

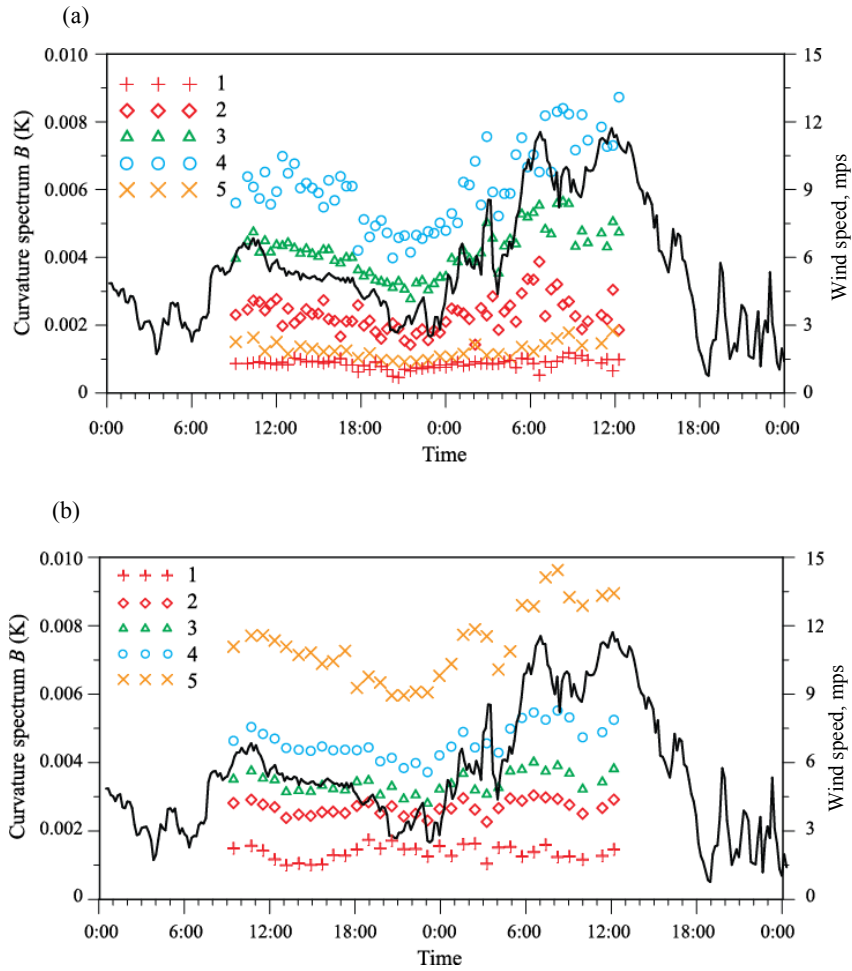


Fig. 6. Temporal course of various components in the curvature spectrum (a) and slope variance (b) on 8–9 June 2005. The black curve shows the near-surface wind speed. The data is presented for five wave numbers, indicated with arrows in Fig. 5.

The oscillations in the sea are probably forced by the atmospheric oscillations as they became evident 10–12 h later. Although the specific dynamics and the origin of the oscillations are yet to be studied, we refer to the similarity between this phenomenon and the instability of the vertical turbulent exchange under stably-stratified conditions, envisaged in [37].

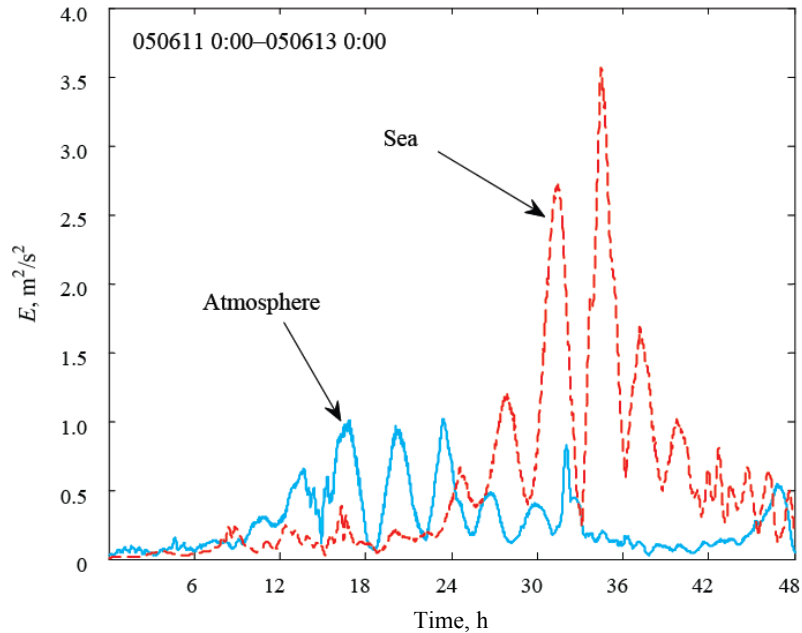


Fig. 7. Quasi-oscillations of the turbulent kinetic energy in the atmospheric boundary layer, calculated by atmospheric friction velocity (blue) and in the surface ocean layer, calculated by rms vertical pulsations (red) during upwelling development in June, 11–13, 2005.

4. SUMMARY

The performed complex measurements from the sea-mounted platform in the coastal zone of the Black Sea, Crimea, Ukraine provided several rich data sets, collected by synchronous observations of the atmospheric micrometeorological parameters, upper ocean turbulence and the state of the sea surface. Specifically, the data have a significant number of samples collected during weak wind and stable stratification conditions, which still have been studied unsatisfactorily in the existing literature. The presented analysis confirmed the main dependences between the surface drag coefficient and meteorological and sea surface parameters, mentioned in earlier publications. However, it was noted that the peculiar behaviour of the surface drag coefficient in the stably-stratified conditions might be an artefact of the classification.

This study demonstrated that the remote radiometric NRRS measurements with a set of microwave radiometers are able to provide reliable and comprehensive information on the state of the sea surface in the range of wavelengths corresponding to the gravity-capillary part of the spectrum.

The data analysis revealed a new regime of air–sea interaction in stably-stratified conditions. In this regime, the turbulent kinetic energy shows substantial quasiperiodic oscillations with a period of about 3.5 h. This oscillation appeared initially in the atmosphere and then in the sub-sea layer with a delay of about 10 h.

ACKNOWLEDGEMENTS

The financial support from the European Research Council, advanced grant FP7-IDEAS, 227915: “Atmospheric planetary boundary layers: physics, modeling and role in Earth system”, from Russian Foundation of Basic Research under grants 11-05-90407, 11-05-00493, 11-02-10007, from the Russian Ministry of Education and Science under contracts 11.519.11.5006, 02.740.11.0676, from the Council on grants of the Russian Federation President under grant No. MK-865.2012.5, by the Russian Government (grant No. 11.G34.31.0078) for research under supervision of the leading scientist and from the programs of the Russian Academy of Sciences were useful for this study.

REFERENCES

1. Sun, J. L., Vandemark, D., Mahrt, L., Vickers, D., Crawford, T. and Vogel, C. Momentum transfer over the coastal zone. *J. Geophys. Res.*, 2001, **106**(D12), 12437–12448.
2. Ozsoy, E., Di Iorio, D., Gregg, M. C. and Backhaus, J. O. Mixing in the Bosphorus Strait and the Black Sea continental shelf: observations and a model of the dense water outflow. *J. Marine Syst.*, 2001, **31**, 99–135.
3. Soomere, T., Myrberg, K., Lepparanta, M. and Nekrasov, A. The progress in knowledge of physical oceanography of the Gulf of Finland: a review for 1997–2007. *Oceanologia*, 2008, **50**, 287–362.
4. Kara, A. B., Metzger, E. J. and Bourassa, M. A. Ocean current and wave effects on wind stress drag coefficient over the global ocean. *Geophys. Res. Lett.*, 2007, **34**, L01604.
5. Kara, A. B., Wallcraft, A. J., Barron, C. N., Hurlburt, H. E. and Bourassa, M. A. Accuracy of 10 m winds from satellites and NWP products near land-sea boundaries. *J. Geophys. Res.*, 2008, **113**, C10020.
6. Grenier, H., Le Treut, H. and Fichefet, T. Ocean-atmosphere interactions and climate drift in a coupled general circulation model. *Clim. Dyn.*, 2000, **16**, 701–717.
7. Smedman, A.-S., Hogström, U. and Bergström, H. The turbulence regime of a very stable marine airflow with quasi-frictional decoupling. *J. Geophys. Res.*, 1997, **102**(C9), 21049–21059.
8. Kuzmin, A. V., Goryachkin, Yu. A., Ermakov, D. M., Ermakov, S. A., Komarova, N. Yu., Kuznetsov, A. S., Repina, I. A., Sadovskii, I. N., Smirnov, M. T., Sharkov, E. A. and Chukharev, A. M. Marine hydrophysical research platform at the Black sea (Katsiveli) as site for remote sensing measurements. *Issledovaniya Zemli iz Kosmosa*, 2009, **1**, 31–41 (in Russian).
9. Repina, I. A., Chukharev, A. M., Goryachkin, Y. N., Komarova, N. Y. and Pospelov, M. N. Evolution of air-sea interaction parameters during the temperature front passage: The measurements on an oceanographic platform. *Atmos. Res.*, 2009, **94**, 74–80.
10. Pospelov, M. N., De Biasio, F., Goryachkin, Y. N., Komarova, N. Y., Kuzmin, A. V., Pampaloni, P., Repina, I. A., Sadovsky, I. N. and Zecchetto, S. Air-sea interaction in a coastal zone: the results of the CAPMOS’05 experiment on an oceanographic platform in the Black Sea. *Atmos. Res.*, 2009, **94**, 61–73.
11. Soloviev, Yu. P. and Ivanov, V. A. Preliminary results of measurements of atmospheric turbulence over the sea. *Phys. Oceanogr.*, 2007, **17**, 154–172.
12. Volkov, Yu. A., Grachev, A. A. and Repina, I. A. Measurements of turbulent frequency spectra in marine surface layer during the calm weather. *Izvestiya Atmos. Oceanic Phys.*, 1993, **29**, 496–500 (in Russian).

13. Grachev, A. A. Free convection frequency spectra of atmospheric turbulence over the sea. *Bound.-Layer. Meteor.*, 1994, **69**, 27–42.
14. Blatov, A. S., Bulgakov, N. P., Ivanov, V. A., Kosarev, A. N. and Tuzhilkin, V. S. *Variability of Hydrological Fields in the Black Sea*. Gidrometeoizdat, Leningrad, 1984 (in Russian).
15. Lovenkova, E. A. and Polonsky, A. B. The climatic characteristics of Crimea coast upwelling and its variability. *Meteorol. Hydrol.*, 2005, **5**, 44–52 (in Russian).
16. Samodurov, A. S., Dykman, V. Z., Barabash, V. A., Efremov, O. I., Zubov, A. G., Pavlenko, O. I. and Chukharev, A. M. “Sigma-1” measuring complex for the investigation of small-scale characteristics of hydrophysical fields in the upper layer of the sea. *Phys. Oceanogr.*, 2005, **15**, 311–322.
17. Chukharev, A. M. Field measurements of turbulent kinetic energy dissipation in sea surface layer. In *Ecological Safety of Coastal and Shelf Zones and Comprehensive Use of Shelf Resources*. Collected scientific papers No. 20 (Ivanov, V. A. et al., eds). NAS of Ukraine, MHI, IGS, OD IBSS. Sevastopol, 2010, **21**, 124–135 (in Russian).
18. Massman, W. J. and Lee, X. Eddy covariance flux corrections and uncertainties in long-term studies of carbon and energy exchanges. *Agricult. Forest Meteorol.*, 2002, **113**, 121–144.
19. Foken, T. *Micrometeorology*. Springer-Verlag, Berlin, Heidelberg, 2008.
20. Sadovsky, I. N., Kuzmin, A. V. and Pospelov, M. N. Wind-wave spectrum parameters investigation based on remote radio-polarimetric measurements. *Issledovaniya Zemli iz Kosmosa*, 2009, **2**, 1–8 (in Russian).
21. Trokhimovski, Y. G. Model of the radiothermal emission of a disturbed sea surface. *Earth Observ. Remote Sens.*, 1998, **15**, 47–61.
22. Kuzmin, A., Pospelov, M. and Trokhimovskii, Yu. Sea surface parameters retrieval by passive microwave polarimetry. In *Microwave Radiometry and Remote Sensing of the Earth's Surface and Atmosphere* (Pampaloni, P. and Paloscia, S., eds). VSP Intern. Science Publishers, Zeist, The Netherlands, 2000, 3–11.
23. Sadovsky, I. N. Wind-wave spectra parameters retrieval method based on measuring angular dependences of the brightness temperature. *Issledovaniya Zemli iz Kosmosa*, 2008, **6**, 1–7 (in Russian).
24. Garratt, J. R. Review of drag coefficients over oceans and continents. *Mon. Weather Rev.*, 1977, **105**, 915–929.
25. Large, W. G. and Pond, S. Open ocean momentum flux measurements in moderate to strong winds. *J. Phys. Oceanogr.*, 1981, **11**, 324–336.
26. Fairall, C. W., Bradley, E. F., Hare, J. E., Grachev, A. A. and Edson, J. B. Bulk parameterization of air–sea fluxes: updates and verification for the COARE algorithm. *J. Climate*, 2003, **16**, 571–591.
27. Mahrt, L., Vickers, D., Frederickson, P., Davidson, K. and Smedman, A. S. Sea-surface aerodynamic roughness. *J. Geophys. Res.*, 2003, **108**(C6), 3171.
28. Kudryavtsev, V. N. and Makin, V. K. Aerodynamic roughness of the sea surface at high winds. *Bound.-Layer. Meteorol.*, 2007, **125**, 289–303.
29. Zilitinkevich, S. S., Hunt, J. C. R., Grachev, A. A., Esau, I. N., Lalas, D. P., Akylas, E., Tombrou, M., Fairall, C. W., Fernando, H. J. S., Baklanov, A. and Joffre, S. M. The influence of large convective eddies on the surface layer turbulence. *Quart. J. Roy. Meteorol. Soc.*, 2006, **132**, 1423–1456.
30. Esau, I. An improved parameterization of turbulent exchange coefficients accounting for the non-local effect of large eddies. *Ann. Geophys.*, 2004, **22**, 3353–3362.
31. Zilitinkevich, S. S. and Esau, I. Resistance and heat transfer laws for stable and neutral planetary boundary layers: old theory, advanced and re-evaluated. *Quart. J. Roy. Meteorol. Soc.*, 2005, **131**, 1863–1892.
32. Peña, A., Gryning, S.-E. and Hasager, Ch. B. Measurements and modelling of the wind speed profile in the marine atmospheric boundary layer. *Bound.-Layer. Meteorol.*, 2008, **129**, 479–495.
33. Sozzi, R., Rossi, F. and Georgiadis, Th. Parameter estimation of surface layer turbulence from wind speed vertical profile. *Environ. Model. Software*, 2001, **16**, 73–85.

34. Fairall, C. W., Grachev, A. A., Bedars, A. and Nishiyama, R. Wind, wave, stress and surface roughness relationships from turbulence measurements made on R/P FLIP in the SCORE experiment. Report, NOAA/ERL/ETL, 1995, 1–28.
35. Donelan, M. A., Haus, B. K., Reul, N., Plant, W. J., Stiassnie, M., Graber, H. C., Brown, O. B. and Saltzman, E. S. On the limiting aerodynamic roughness of the ocean in very strong winds. *Geophys. Res. Lett.*, 2004, **31**, L18306.
36. Chukharev, A. M. and Repina, I. A. Sea and atmospheric boundary layers interaction on small and middle scale in coastal zone. *Phys. Oceanogr.*, 2012, **22**. Forthcoming.
37. McNider, R. T., Shi, X., Friedman, M. and England, D. E. On the predictability of the stable atmospheric boundary layer. *J. Atmos. Sci.*, 1995, **52**, 1602–1614.
38. Apel, J. R. An improved model of the ocean surface wave vector spectrum and its effects on radar backscatter. *J. Geophys. Res.*, 1994, **99**, 16269–16291.
39. Elfouhaily, T., Chapron, B., Katsaros, K. and Vandemark, D. A unified directional spectrum for long and short wind-driven waves. *J. Geophys. Res.*, 1997, **102**, 15781–15796.
40. Romeiser, R., Alpers, W. and Wisman, V. An improved composite surface model for the radar backscattering cross section of the ocean surface 1. Theory of the model and optimization/validation by scatterometer data. *J. Geophys. Res.*, 1997, **102**(C11), 25237–25250.

Mere ja atmosfääri vastasmõjust nõrkade ning mõõdukate tuulte puhul Musta mere rannikuvööndis

Irina Repina, Arseny Artamonov, Alexander Chukharev, Igor Esau,
Yury Goryachkin, Alexey Kuzmin, Michael Pospelov, Ilya Sadovsky
ja Mikhail Smirnov

On esitatud Musta mere Krimmi (Ukraina) rannikust umbes 600 m kaugusel ligikaudu 30 m sügavuses vees šelfinõlval paikneval uurimisplatvormil kevaditi ja sügiseti 2005–2011 läbi viidud mere ning atmosfääri vastasmõju mõõtmiste tulemused. Keskenduti vastasmõju analüüsile nõrga ja mõõduka tuule ning süva-veekerke kombinatsiooni tingimustes, kasutades nii kontaktmõõtmisi kui ka kaugseire võimalusi. Turbulentsi omadusi hinnati traditsioonilise keerisvoo analüüsi meetoditega ja radiopolarimeetriaal tuginevate uudsete seadmetega. On näidatud, et pinnatakistuse koefitsient sõltub oluliselt vee- ja õhutemperatuuride vahest isegi nõrga tuule korral. On näidatud, et eksisteerib senitundmatu mere ja õhu vastasmõju režiim, mida iseloomustavad algul atmosfääri turbulentsi parameetrite 3,5-tunnise intervalliga kvaasiperioodilised muutused ning ligikaudu 10–12 tunni möödumisel tekkivad samalaadilised muutused mere pinnakihis. Radiopolarimeetriaalsete mõõtmistega on määratud kapillaarlainete omadused kirjeldatud režiimi vältel.